Improving Parameter Estimates Obtained from Thermal Response Tests: Effect of Ambient Air Temperature Variations

T.V. Bandos[1*], Á. Montero[2], P. Fernández de Córdoba[1], J.F. Urchueguía[1]

[1] *Instituto Universitario de Matemática Pura y Aplicada, Universidad Politécnica de Valencia, Camino de Vera s/n, 46022 Valencia, Spain*

[2] *Instituto de Ingeniería Energética, Universidad Politécnica de Valencia, Camino de Vera s/n, 46022 Valencia, Spain*

ABSTRACT

This paper presents a method of subtracting the effect of atmospheric conditions from thermal response test (TRT) estimates by using data on the ambient air temperature. The method assesses effective ground thermal conductivity within 10% of the mean value from the test, depending on the time interval chosen for the analysis, whereas the estimated value can vary by a third if energy losses outside the borehole are neglected. Evaluating the same test data using the finite line-source (FLS) model gives lower values for the ground thermal conductivity than for the infinite line-source (ILS) model, whether or not heat dissipation to ambient air is assumed.

Keywords: Borehole heat exchangers, Heat transfer, Finite line-source method, Ground-source heat pumps, Thermal response test

*Corresponding author. Tel.: +34 963877007/85247. E-mail address: tbandos@uv.es.

Nomenclature

$C(C_f)$	volumetric heat capacity of ground (fluid) ($Jm^{-3}K^{-1}$)
D	length along the piping between the temperature probe location and the borehole inlet or outlet (see **Fig. 1**) (m)
Ei	exponential integral
$g(t) = \frac{2\pi\lambda}{q_z}(T - T_0)$	thermal response function
G	fluid volume flow rate (m^3s^{-1})
H	depth of the borehole heat exchanger (BHE) (m)
r	radial coordinate (m)
$p =< Qair > /Qt$	part of the total heat rate transmitted to the ambient air
r_b	radius of the BHE (m)
R_a	thermal resistance between fluid and ambient air (KmW^{-1})
R_b	borehole thermal resistance (KmW^{-1})
$q_z = \frac{GC_f}{H}(T_{in} - T_{out})$	heat flow per unit length (Wm^{-1})
Q_{air}	heat dissipation rate to the ambient air (W)
$Q_t = GC_f(T^*_{in} - T^*_{out})$	total produced heat rate (W)
s	coordinate along the pipe in the range from 0 to D (m)
t_0 (t_1)	start (end) point of the time interval (s)
$t_r = r_b^2/\alpha$	short time scale for the BHE (s)
$t_s = H^2/(9\alpha)$	Eskilson (1987) steady-state time scale (s)
$t_z = H^2/\alpha$	large time scale for the BHE (s)
T	temperature of ground (K or °C)
T_a	ambient air temperature (K or °C)
T_f	temperature of heat carrier fluid (K or °C)
T_0	undisturbed ground temperature (K or °C)
T_{in}	inlet temperature of BHE (K or °C)
T_{out}	outlet temperature of BHE (K or °C)
T^*_{in}	measured inlet temperature of BHE (K or °C)
T^*_{out}	measured outlet temperature of BHE (K or °C)

z	vertical axial coordinate (m)

Greek letters

$\alpha = \lambda/C$	ground thermal diffusivity (m^2/s)
γ	Euler's constant
λ	ground thermal conductivity ($W(Km)^{-1}$)
$\eta[= D/(R_a C_f G)]$	dimensionless parameter

Superscripts

$\overline{.....}$	arithmetic mean
$< ... > (= \int_0^H .....dz/H)$	integral mean
$<...>_t$	time average
$...\uparrow (... \downarrow)$	up (down) directions for heat carrier fluid circulation

Subscripts

a	ambient air

1. Introduction

Nowadays, ground-source heat pumps (GHPs) are a solid alternative as choice of system for heating and cooling in buildings (Omer, 2008; Sanner et al., 2005; Urchueguía et al., 2008). By comparison with standard technologies, they offer competitive levels of comfort, reduced noise levels, savings of greenhouse gas emissions, and reasonable environmental safety. Furthermore, their electrical consumption and maintenance requirements are lower than those required by conventional systems and, consequently, the annual cost is lower (Lund, 2000). Ground-source systems are recognized by the Environmental Protection Agency as being among the most efficient and comfortable heating and cooling systems available today.

A thermal response test (TRT) is a method of determining the effective on-site ground thermal conductivity in order to design ground coupled heat pump systems. These in-situ tests are based on the ILS theory of heat transfer by thermal conduction (Ingersoll et al., 1954; Reuβ et al., 2009). Due to its two-dimensional nature, the ILS theory cannot describe axial temperature variations around geothermal borehole heat exchanger.

Fig. 1 represents a typical TRT test to measure the temperature response of the borehole heat exchanger (BHE) to a constant heat injection or extraction. A U-tube loop, through which a heat carrier fluid circulates, is inserted inside the borehole to approximately the same depth as the BHE planned for the site. To provide a constant heat flux to the ground, the fluid flow rate in the borehole loop and the temperature difference between inlet and outlet are kept constant during the testing. The outputs of the TRT are the inlet (T_{in}) and outlet (T_{out}) temperatures of the heat carrier fluid as a function of time (see **Fig.1**). The difference between the temperatures T_{in} and T_{out}, measured at the end points of the U-tube, is used to determine the rate at which heat is transferred by thermal conduction into the ground.

The BHE, which consists of two tubes separated by filling material, can be modeled as a heat source in the form of a line or cylinder. The effective thermal resistance of the borehole (Mogensen, 1983) defines the temperature drop between the BHE surface and an average temperature of the fluid. The temperature of heat carrier fluid circulating through the loop varies with depth, as do the ground thermal properties. A weighted average of T_{in} and T_{out} measured at the end points of the U-tube is assumed to be the mean temperature of the heat carrier fluid over the loop length (Marcotte and Pasquier, 2008). Typically, their arithmetic average is compared with a reference temperature of the borehole surface from the ILS model, around which the TRT is designed. From these experimental data and with an appropriate model for average temperature around the BHE, the effective thermal conductivity of the surroundings is inferred.

Different analytical and numerical methods have been developed for determining ground thermal properties from the TRT output data. The cylinder heat source (Ingersoll et al., 1954) and line heat source (Carslaw and Jaeger, 1959) model for BHE with parameter-estimating techniques are commonly applied in Europe (Claesson and Eskilson, 1988; Gehlin and Hellström, 2003; Sanner et al., 2005; Witte et al., 2002) and North America (Austin, 1998; Beier and Smith, 2002; Beier, 2008; Shonder and Beck, 2000). Kelvin's ILS model is among the most widely used models for evaluation of response test data at sufficiently large times because of the fact that the TRT was actually devised on the basis of ILS theory (Ingersoll et al., 1954; Mogensen, 1983).

The FLS model overcomes some limitations of the ILS model: its solution has been expressed as an integral (Eskilson, 1987), given zero temperature at the boundary of the semi-infinite medium. The temperature response functions, so-called "*g*-functions" introduced by Eskilson (1987), are based on the solution of this model for the BHE temperature field at a constant heat load. The *g*-functions are computed for moderate times (Javed et al., 2009) and provide an asymptotic approach to the steady-state limit, which is not reached within the ILS model. The FLS solution for the ground temperature in the vicinity of the midpoint of the BHE depth was shown to be approximately the same as the classical result of the traditional ILS during the TRT (Bandos et. al, 2009).

However, the best solution for applications is given by the mean integral temperature (Lamarche and Beauchamp, 2007; Zeng et. al, 2002). This is because the average or effective thermal properties of the ground are used in the design. An exact solution for the temperature averaged over the borehole depth has been approximated, providing analytical formulae for a wide time range (Bandos, et al., 2009) that account for the edge effects due to the vertical heat transfer along the borehole. These simple asymptotic expressions for the mean borehole temperature allow flexibility in parametric analysis of the test data. It is important to take account of the finite depth of the BHE because there is an incentive to install the minimum possible length and so decrease the cost of the ground source systems.

Evaluating TRT data based on the ILS model assumes that there is no heat transfer between the heat carrier fluid and the ambient air, and that there are no significant effects of boundary conditions for the vertical temperature profile in the ground surrounding the BHE. In practice, the inlet and outlet temperatures T^*_{in} and T^*_{out} are measured at some distance D from the ground surface; Fig.1 shows location of the temperature probes. The data analysis is based on solution of a purely conductive problem in the ground, which depends on T_{in} and T_{out} temperatures inferred from T^*_{in} and T^*_{out} (see **Fig.1**). The above-surface part of the TRT system is thermally insulated. However, it is difficult to insulate the external pipes completely; the exchange of heat between the ambient air and fluid is often inevitable. Depending on air temperature, the heat carrier fluid can gain or lose some heat to the ambient. Furthermore, even a small flow of heat through the

insulation may influence the ground conductivity estimate, causing instability (i.e., the dependence of the estimate on the time interval used for evaluation). That complicates the analysis of the TRT.

Experiments have demonstrated that the evaluation of thermal conductivity is affected by ambient air temperature changes. The influence of diurnal temperature changes on the measured fluid temperature has been reported several times (Austin, 1998; Esen and Inalli, 2009; Florides and Kalogirou, 2008; Fujii et al., 2009; Signorelli et al., 2007). In particular, the cooling effect of the ambient conditions has been observed (Gehlin and Nordell, 2003). The observation of atmospheric effects in numerous experiments prompts a quest for a method that would allow the influence of air temperature variation to be subtracted from the dependence of the ground conductivity estimate on the time interval chosen for analysis. Being complementary to the efforts to increase the accuracy of the test (Sanner et al., 2005; Witte et al., 2002) such a technique would allow the already existing data, whose acquisition is fairly costly, to be used more efficiently.

This paper addresses the heat transfer in the above-ground and subsurface parts of the TRT system shown in **Fig. 1**. It presents (i) a new method for subtracting the atmospheric effect on the test parameters by using data of ambient air temperature in the estimation; (ii) analysis of test data on the basis of the formula for average borehole temperature, accounting for the edge effects from the FLS model; and (iii) comparison of these thermal conductivity estimates to those from the ILS model, accounting for heat losses to the ambient.

The rest of the paper is organized as follows: Section 2 reviews the results from the classical infinite and finite line-source models. Section 3 introduces the heat balances for the heat carrier fluid and proposes a method to account for climatic influence and efficiently subtract it from the data. Section 4 compares the proposed model with experimental dependence of the temperature of the circulating fluid on time and summarizes results for the test estimates with and without heat losses to the atmosphere. Finally, Section 5 concludes and discusses directions for further investigation.

2. Line-source theory

Within the ILS framework commonly applied for the evaluation of thermal response test data, the ground is assumed to be a homogeneous infinite medium characterized by its thermal conductivity λ. In the vicinity of the borehole, for sufficiently large time values, the ILS model gives (Ingersoll et al., 1954):

$$T(r,t) = T_0 - \frac{q_z}{4\pi\lambda} Ei\left(-\frac{r^2}{4\alpha t}\right)$$

$$\approx \frac{Q_z}{4\pi\lambda}\left\{\ln\frac{4\alpha t}{r^2} - \gamma + O\left(\frac{r^2}{4\alpha t}\right)\right\} + T_0, \qquad for\ \frac{4\alpha t}{r^2} >> 1 \qquad (1)$$

where *Ei(u)* denotes the exponential integral (Carslaw and Jaeger, 1959) q_z as the heat flux density per length unit, γ as Euler's constant, α as ground thermal diffusivity, and T_0 as the undisturbed ground temperature. It is usually assumed that the heat is released at a constant rate from the BHE, in the "radial" direction orthogonal to it, and is transferred by the mechanism of thermal conduction. The ILS solution is applicable to the temperature around a midpoint of BHE, modeled as an FLS of the same constant heat flow, and only for moderate times ($t < t_z$) (because a physically reasonable steady-state solution is beyond its scope). It has been shown

analytically that the classical result of the traditional ILS is reproduced by the FLS solution for the ground temperature about the midpoint depth (up to the exponentially small correction terms $e^{-t_z/t}$) at times that are comparable with the duration of the TRTs (Bandos et. al, 2009). That is precisely the reason why the simplifying assumption about an infinitely long heat source in an infinite medium provides a good approximation and is commonly used for the TRT analysis (Mogensen, 1983) and for the design standards of the International Ground Source Heat Pump Association (Bose et al., 1985). This is also why the ILS is used as a benchmark model for comparison with new proposals.

Approximate expressions for average borehole temperature (instead of temperatures at the midpoint of the borehole) were derived to apply over a wide range of time values (Bandos et. al, 2009). In the frame of the FLS in the semi-infinite region, the approximation of the average ground temperature for the times corresponding to the TRT (i.e., for $t_z >> t >> r^2/4\alpha$) is given by:

$$< T(r,z,t) - T_0 >= \frac{q_z}{4\pi\lambda}\left\{ ln\frac{4\alpha t}{r^2} - \gamma - \frac{3}{\sqrt{\pi}}\sqrt{\frac{4t}{t_z}} + \frac{3r}{H} - \frac{3}{\sqrt{\pi}}\frac{r^2}{H^2}\sqrt{\frac{t_z}{4t}}\right\}$$

$$< T(r,z,t) - T_0 >= \frac{1}{H}\int_0^H (T(r,z,t) - T_0)dz \qquad (2)$$

This expression for the average temperature of the BHE differs from the classical one (**Eq. 1**) by the finite-size corrections, which vanish in the limiting case of $H \to \infty$. Notice that for both models ILS (1) and FLS (2), the heat flux density q_z is implied to be the same and constant along the borehole, assuming a purely conductive heat transport. The effects of the finite source size are described by the last three terms in the right-hand side of **Eq. 2**. Their contribution to the transient temperature at various radial distances from the borehole center is significant for shallow boreholes as calculated numerically (Philippe et al., 2009). Indeed, **Eq. 2** shows that, for H = 25m and for $t/t_z \approx 0.16$ and $t/t_z \approx 0.0016$, corresponding approximately to 4 months and 1 day respectively, the relative difference between the results from the ILS and FLS model reaches 30% and 6.5% at r = 1m.

Early time, $t < 5t_r$, values are in the order of one day (Eskilson, 1987), whereas typical thermal test durations range from 40 to over 200 hours (Signorelli et al., 2007). The latter fall within $t_r < t < t_z$, termed medium times to distinguish them from very long time values $t > t_z$ corresponding to the approach to the steady-state (Claesson and Eskilson, 1988). In this case, the integral average temperature change at the radial distance r from the borehole center is given by (Bandos et al., 2009):

$$\frac{q_z}{4\pi\lambda}\{4\sinh^{-1}\frac{H}{r} - 2\sinh^{-1}\frac{2H}{r} + 3\frac{r}{H} - 4\sqrt{1+\frac{r^2}{H^2}} + \sqrt{4+\frac{r^2}{H^2}} - \frac{t_z^{3/2}}{12\sqrt{\pi}t^{3/2}}(1 - \frac{3t_z\ (1+r^2/H^2)}{20t})\}, \quad t >> \max(H^2, r^2) \qquad (3)$$

where $\sinh^{-1} a = \ln(a + \sqrt{1+a^2})$.

Eq. 3 describes the time-asymptotic approach to the steady-state temperature of the designed geothermal system, whereas **Eq. 2** is applicable to the data of the test within the medium time interval. The following section shows how to account for the atmospheric effect that influences the time dependence of the temperature of heat carrier fluid.

3. Analysis of TRT data

3.1 The response test

The test described here was carried out in Castellon (Spain) in January 2007, to obtain design values for the planned geothermal pump. In the data acquisition system, the apparatus used to monitor the thermal response was connected to the BHE by thermally insulated 4-m-long tubes. The field test was performed on a borehole with radius r_b of 0.15m, and H = 25m (See Fig. 1). Bentonite grout filled the space between the U -loop tube and the inner BHE wall, and water was used as the heat carrier fluid. By measuring the plug flow temperature before the test, the undisturbed temperature was determined to be 18.4± 0.2°C.

The test apparatus worked in heat injection mode: the water entering the BHE was warmer than that exiting. The test parameters were monitored every three minutes by a data logger. **Fig 2** presents plots of the 1,418 data readings of ambient air temperature and average water temperature, defined by the arithmetic mean of the inlet and outlet temperatures, as a function of time during the 71-hour experiment.

To provide a constant heat rate (about 1.04 kW, as shown by the gray line of **Fig. 3**), the difference between the temperatures of the circulating fluid at the input and output of the ground loop was held constant (at about 3°C), as was the volume flow rate of water, $G \approx 0.3$ m^3/h. High-frequency oscillations of the total heat rate were due to the control system for the temperature of water entering borehole. The flow rate was measured by a Coriolis meter with an accuracy limited to 1%, while the temperature sensors were four-wire PT100 with an accuracy of ±0.1°C.

Although pipes connecting the test device with the borehole were well thermally insulated, an undesirable correlation between the air temperature and the mean temperature of the fluid was also observed in our test, as in other cases. Just visible in **Fig. 2** are small jumps in average water temperature at 15, 30, and 54 hours that are related to significant variations of the temperature of the ambient air around its average value of 14°C. This implies some heat transfer through the above-ground pipes between the borehole and data acquisition instrument (Sanner et al., 2005).

The relationship between the time dependence of the carrier fluid temperature and the ambient air temperature has been observed during TRTs carried out by different groups (Esen and Inalli, 2009; Florides and Kalogirou, 2008; Fujii et al., 2009; Gehlin and Nordell, 2003; Sanner et al., 2005; Shonder and Beck, 2000; Signorelli et al., 2007; Spitler, 2000). This may indicate that it is often difficult to completely remove the atmospheric effect by means of insulation. The fact that, in practice, the ambient air and the fluid temperatures are correlated strongly affects the stability of the ground conductivity estimate, making it dependent on the chosen time interval (Austin, 1998; Gehlin and Hellström, 2003; Shonder and Beck, 2000; Signorelli et al., 2007; Witte et al., 2002). On the other hand, the observation of such correlations in numerous experiments suggests that it is necessary to consider heat transfer processes in the geothermal system as a whole in order to handle test data that is influenced by the ambient air temperature variation.

3.2 Climatic effect on the heat transferred to the ground: interpretation model

Heat exchange between the ambient air and the fluid in the above-ground pipe work changes the heat transferred to the borehole. Then, the total heat rate Q_t can be written as a sum of the heat dissipation rate to the ambient air (Q_{air}) and the actual heat rate transferred to the ground (q_zH):

$$Q_t = Q_{air} + q_zH \tag{4}$$

Besides diurnal variations of the air temperature, the interior temperatures of the test rig affect the efficiency of the system operation (Sanner et al., 2005). In many practical circumstances, the inlet and the outlet temperatures are measured using temperature probes on the above-ground connection pipes, as implied in **Fig. 1**. The thermal influence on the borehole temperature of the heat carrier fluid in the above-ground piping has been recorded (Gehlin and Nordell, 2003).

The fluid temperature changes with the s coordinate along the pipes outside the borehole due to the undesirable heat exchange with the ambient air. In the quasi steady-state case, the heat transport by the fluid in the tube, accompanied by the transverse heat flux to the air, is governed by the convection equations (Claesson and Eskilson, 1988; Hellström, 1991):

$$GC_f \frac{dT_f^{\downarrow}(s,t)}{ds} = (T_a(t) - T_f^{\downarrow}(s,t))/R_a, \qquad T_f^{\downarrow}(s=0) = T_{in}^* \tag{5}$$

$$-GC_f \frac{dT_f^{\uparrow}(s,t)}{ds} = (T_a(t) - T_f^{\uparrow}(s,t))/R_a, \qquad T_f^{\uparrow}(s=0) = T_{out}^* \tag{6}$$

$$0 \le s \le D$$

The measured temperatures T^*_{out} and T^*_{in} related to the borehole input and output are required to estimate the total amount of the heat rate:

$$Q_t = C_fG(T^*_{in} - T^*_{out}) \tag{7}$$

Heat dissipation to the ambient air causes temperature variation along the connection pipe. As a result, the actual heat rate transferred to the ground is not Q_t, but q_zH (see **Eq. 4**). In fact, the heat convection by fluid balances the radial heat flux to the ground and determines the heat rate q_zH through the temperatures near the surface level as:

$$q_zH = C_fG(T_{in} - T_{out}) \tag{8}$$

The BHE input and output temperatures, $T_{in} = T^{\downarrow}_f\,(s = D)$ and $T_{out} = T^{\uparrow}_f\,(s = D)$, need to be found. Here, D is the length of piping along the zone of thermal contact of fluid with the ambient air (i.e., between the point of measurement and the point of input (output) to the BHE, as **Fig. 1** shows). The effective length D may also include the uppermost part of the borehole.

The solution of the system of **Eq. 5** and **6** with the boundary conditions at the points of measurement can be written as:

$$T_{in} = T_{in}^* e^{-\eta} + T_a(1 - e^{-\eta}) \tag{9}$$

$$T_{out} = T^*_{out} e^{\eta} + T_a(1 - e^{\eta})$$

$$\eta = D/(R_a C_f G) \tag{10}$$

The above solutions depend on thermal characteristics of the flow system through the model parameter η. Its physical meaning can be inferred from physical parameters entering **Eq. 10**: flow rate, heat capacity of fluid, piping dimensions; its value can be calculated based on an assumed thermal resistance R_a. Notice that this model parameter η takes non-zero values in actual conditions of penetrating ambient influence, while its zero value is reached for the limiting case of perfect thermal insulation of the connecting pipes $R_a = \infty$ or $G \to \infty$. Therefore, $\eta = 0$ corresponds to the ideal test conditions without heat dissipation to the ambient and is used for comparison with the proposed model hereafter. A non-zero value of the dimensionless parameter η from **Eq. 10** accounts for the climatic influence. It can be calculated using physically observable properties, as in **Eq. 10**, or estimated from the test data as described below.

The outputs of the exterior problem, **Eq. 9**, influence both the heat rate to the ground and mean fluid temperature. Indeed, substituting **Eq. 9** into **Eq. 8**, one finds:

$$q_z(\eta, t)H = C_f G(2T_a(t)\sinh\eta - e^{\eta}T^*_{out} + e^{-\eta}T^*_{in}) \tag{11}$$

and then

$$\overline{T_f}(\eta, t) = (T_{out}(t) + T_{in}(t))/2 = T_a(t)(1 - \cosh\eta) + (e^{\eta}T^*_{out} + e^{-\eta}T^*_{in})/2 \tag{12}$$

The inputs for the conduction problem, related to T_{in} and T_{out} at the top of the borehole are now expressed using measured fluid temperatures T^*_{in} and T^*_{out}.

Notice that if the connecting pipes were ideally insulated (i.e., $\eta = 0$, neither T_{out}, T_{in}, or q_z would depend on the ambient air temperature. In the test, the temperature probes are to be immersed directly into the flow (Witte et al., 2002), where, presumably, the outside heat influence should not penetrate. However, under real conditions, there exist heat losses to the ambient outside the borehole, and so the parameter η takes small but non-zero values.

The question then arises of how to select parameter η in order to filter out the effect of air temperature variation. The energy rate balance, **Eq. 7** and **11** set the correspondence between η and the fraction p of the total heat rate transmitted to the ambient air

$$< Q_{air} >_t = p < Q_t >_t \tag{13}$$

as:

$$(p - 1 + \cosh\eta)\langle T^*_{in}(t) - T^*_{out}(t)\rangle_t = \langle T^*_{out}(t) + T^*_{in}(t) - 2T_a(t)\rangle_t \sinh\eta \tag{14}$$

Note that the thermal resistance $R_a = D/(\eta C_f G)$ between the fluid and the air is independent of the flow direction due to the fact that above equation is invariant under $\eta \to -\eta$ if this is supplied by $T^*_{in}(t) \leftrightarrow T^*_{out}(t)$. If the heat loss to the ambient air is a small part of the total produced heat rate ($p << 1$), the leading terms in the series expansion in η in **Eq. 14** give:

$$\eta = p\frac{\langle T^*_{in}(t) - T^*_{out}(t)\rangle_t}{\langle T^*_{out}(t) + T^*_{in}(t) - 2T_a(t)\rangle_t} \tag{15}$$

Then, the values of η turn out to be small as long as $p << 1$; these parameters are proportional, and the case of $\eta = 0$ corresponds to $p = 0$. (**Eq. 15** does not mean that the flow parameter should be considered as a function of the measured temperatures.) One can use **Eq. 15** to select η.

The idea behind the proposed method of handling TRT data is to use the freedom in choosing η to suppress the influence of the air temperature oscillations. The algorithm to determine the model parameter η can be summarized as follows:

1. Choose an initial guess for p (for instance, use an acceptable energy loss to the ambient, and calculate η from **Eq. 15**
2. Apply the three-parameter scheme, described in section 4.1 below, varying estimates of λ, R_b, and T_0
3. Compare the value T_0 thus obtained with the experimental value T_0^{exp}
4. If $T_0 - T_0^{exp}$ is less than some tolerance threshold, then stop iteration: the value of η is sufficiently accurate; otherwise, choose another value for p

As a sample application of the above proposed algorithm for determining η using T_0^{exp} , consider the TRT data. For the initial guess of p, the optimal choice happens to be $p = 0.055$, or 5.5% of heat dissipated to the ambient during the heat injection. With this value for p, **Eq. 15** gives $\eta = 0.006$. Then, as a result of steps 2 and 3, the estimate of T_0 (what is the value) appears to be close enough to the value T_0^{exp} determined from the experiment before the test.

Fig. 3 plots the variable heat rates $q_z H$ and Q_{air} calculated using **Eq.11** and **17** with $p = 0.055$, $\eta = 0.006$; it is seen that the heat rate Q_t remains roughly the same by keeping the temperature difference $T^*_{in} - T^*_{out}$ constant during the TRT. There are minor variations of the resulting heat input during this TRT (in accordance to hardly discernable fluctuations of fluid temperature caused by the daily air temperature fluctuations; see **Fig. 2**.)

In the next stage, the total heat flow from the fluid to ground through the borehole wall is considered. When fitting the temperature at the lateral surface of the borehole $T_b = T(r = r_b, t)$ to the experimental data $\overline{T_f}$ for the mean heat carrier temperature, the thermal resistance R_b between the borehole wall and the fluid must be taken into account (Mogensen, 1983):

$$R_b C_f G(T_{in} - T_{out}) = R_b(Q_t - Q_{air}(t))/H = \overline{T_f}(\eta, t) - T_b(t) \qquad (16)$$

Notice that the temperature drop, $T_f(\eta, t) - T_b(t)$, is influenced by the ambient air temperature $T_a(t)$ through the heat rate $Q_{air}(t)$ that is given by:

$$Q_{air}(t) = C_f G(\sinh\eta(T^*_{in} + T^*_{out} - 2T_a(t)) + (1 - \cosh\eta)(T^*_{in} - T^*_{out})) \qquad (17)$$

or, for small values of η (<< 1):

$$Q_{air}(t) \approx 2\eta C_f G(\overline{T_f}(\eta, t) - T_a(t)) \qquad (18)$$

Besides determination of the ground thermal conductivity, an evaluation of the borehole thermal resistance, R_b, is another objective of the test. This test estimate is very sensitive to the value of undisturbed temperature T_0 (Marcotte and Pasquier, 2008).

The proposed formulae for subtraction of climatic influence from the TRT data, using a multivariate parameter estimation analysis, is described in the next section and the results are compared with the test estimates from new models.

4. Results and discussion

4.1 Parameter estimation algorithm

The data obtained from the TRT are evaluated and compared by making use of the ILS and FLS models, along with the above described method of accounting for the heat rate transmitted to ambient air, characterized by η. To find suitable model parameters, **Eq. 1** and **2** (in the time interval of their validity) have been matched, using a regression technique, to the experimental data for the mean temperature of the water as a function of time.

Parameter estimation minimizes some measure of discrepancy between the measured fluid temperature $\overline{T_f^{exp}}$ and its prediction from **Eq. 16**, which can be rewritten as:

$$\overline{T_f}(t) = \langle q_z(t) \rangle_t \frac{g(t)}{2\pi\lambda} + q_z(t) R_b + T_0 \qquad (19)$$

Here, $< ... >_t$ denotes time averaging, and the *g*-function is defined by the models in **Eq. 1** and **2**. To find optimal test estimates, the measure of loss, which is proportional to the error $\overline{T_f} - \overline{T_f^{exp}}$, is minimized by adjusting test parameters. The model parameter η was fixed by applying two or three parameter schemes based on the multivariate regression method. In the three-parameter estimation procedure, T_0 was allowed to vary, along with the variables of the two-parameter scheme: ground thermal conductivity and borehole thermal resistance.

Note that the approximation for the average temperature in **Eq. 2** differs from the linear logarithmic time dependence for the ILS (**Eq. 1**) by the extra terms that are proportional to 1/H. Both approximate functions remain linear in the test parameters $1/\lambda$, R_b, and T_0. However, the general regression technique is valid regardless of the functional form of the time dependence of the model (Hastie et al., 2001). The optimization procedure was performed using the best estimates of the three or two variables (i.e., variable or fixed T_0) for both the model proposed here, $Q_{air}(\eta \neq 0) \neq 0$, and the traditional version, $Q_{air}(\eta = 0) = 0$ (i.e., with and without energy loss in the connections).

4.2 Test parameter estimates with four models

Fig. 4 compares the results of FLS and ILS models with the results of the benchmark ILS model, $q_z(\eta = 0)$, using $\alpha = 1.21 \times 10^{-6} m^2/s$ throughout the numerical calculations. Four different models were developed from the data measured (in situ) by applying two- and three-parameter estimation methods. These are FLS and ILS for $\eta = 0$ and FLS and ILS for $\eta \neq 0$ models: i.e., two models incorporating measured temperatures of the ambient air, $q_z(\eta \neq 0)$, and two models without it, $q_z(\eta = 0)$.

The classical ILS and FLS approaches are applied to the data set obtained from the test after the first few hours. Transient early-time data ($t << r_b^2/\alpha$) are influenced by the borehole itself (i.e., by its radius, length, etc.), thermal properties of the grout, tubes, and convective resistance between inside their walls and the fluid. Therefore, these early-time data are ignored in the analysis of the thermal properties of ground.

Fig. 4 shows the thermal conductivity as a function of length of the time interval $[t_0, t_1]$ chosen for the estimation, where t_0 is the time the measurement starts and t_1 is the overall time of the measurement. Then, the length of the estimation interval $(t_1–t_0)$ corresponds to time on the x-axis of **Fig. 4** and **6**.

Fig. 4 plots the thermal conductivity estimates obtained by using the data in the intervals: from the [46–71] hours to the [1–71] hours (thus, t_0 varies from 1 hour to 46 hours). The length of estimation interval is changed by 1 hour in a step-wise manner from 25 to 70 hours; the former interval corresponds to the late times of the test. These sequential plots can indicate whether the estimate converges to a particular value over the time intervals chosen for the analysis and provides a check for groundwater flow (Sanner et al., 2005).

Firstly, **Fig. 4** compares the thermal conductivities on different length-of-time intervals estimated from both the ILS and FLS models for $\eta = 0$ (i.e., assuming zero energy losses to the ambient air) for the same test. When assuming no heat losses in the above-ground piping and the uppermost part of the vertical BHE, the instability of the effective thermal conductivity may mask a convergent value of the TRT estimate. Indeed, **Fig. 4** reveals the cyclic nature of the temperature response for $\eta = 0$ because of the influence of the outside perturbation; very small and hardly noticeable changes in the mean fluid temperature curve in **Fig. 2** are significantly amplified for λ, which is inversely proportional to its time derivative.

As **Fig.4** demonstrates, conventional data analysis (i.e., assuming no heat exchange between the ambient air and the fluid) gives significant differences between thermal conductivity estimates within the selected time intervals (when varying t_0 from 1 hour to 46 hours, while t_1 is fixed). In contrast to this TRT estimate, which is hardly interpretable, one can find convergence if the heat exchange through the connection pipes is taken into account by setting a non-zero value for the parameter η (see **Eq. 10**). And if the model accurately represents the heat transfer processes in the whole system, the thermal conductivity curves are expected to flatten out below and above the ground surface for large estimation intervals .

Secondly, **Fig. 4** compares the λ values estimated from both the ILS and FLS models, for $\eta = 0.006$, on different time intervals from the same test data. In this case, the injected heat rate varies with time, but without clear decreasing or increasing trends that can distort the estimate of ground conductivity (Beier and Smith, 2003). A superposition technique or a method proposed by Beier and Smith (2003) can provide a solution for the case of non-constant heat flow. However, if q_z weakly changes with time, $\Delta q_z/q_z << 1$, acceptable results can also be obtained through averaging the heat load over the TRT time. This is just the case, because the maximum variation of q_z (caused by the ambient temperature variations) is less than 5.5% of average heat flow. Therefore, to fit the model to the water temperature data, when the variations of $q_z(\eta;t)$ are caused by T_a (t) fluctuations, the average component of the heat rate density, $< q_z(\eta;t) >_t$, is used. As can be seen from **Eq. 19**, the mean heat rate is the key factor in the g-function, whereas the time variation of $q_z(\eta;t)$ accounts for the atmospheric effect which it turns out to be proportional to the time dependence of the air temperature attenuated by the small multiplier η in Eq. 18 and is therefore small. In this case, $\eta \neq 0$, **Fig. 4** also demonstrates that the ground conductivity curve

approaches a horizontal line with increasing length of time series. In addition, these sequential plots in **Fig. 4** allow assessment of the time interval that is necessary to obtain an accurate parameter estimate. **Fig. 4** shows that fluctuations in ground thermal conductivity estimates from the both ILS and FLS models with $\eta = 0$ almost disappear when using three-parameter regression for the value of $\eta \neq 0$ determined previously. Indeed, as **Fig. 4** demonstrates, the effective ground thermal conductivity estimate from the ILS (FLS) is constant to within 10%.

Fig. 5 shows that the FLS temperature curve ($\eta \neq 0$) (solid line) calculated in such a way (with the converged values of the test estimates found by using the three-parameter scheme) lies perfectly on a line of the measured temperature of fluid (ignoring high frequency fluctuations). This excellent agreement between the two curves is reached by taking into account the rate of heat losses $Q_{air}(t)$. The temperature curve (solid line) with the underlying atmospheric trend corresponds to $\lambda = 2.57$ W/(m°C) and $R_b = 0.174$ m°C/W, $T_0 \approx 18.32$°C, estimated from the three-parameter scheme for the proposed model with $\eta = 0.006$ in the time interval range from 6 to 71 hours. The straight dashed line in **Fig. 5** corresponds to a thermal conductivity of 2.66 W/(m°C) and borehole resistance of 0.163 m°C/W found from two parameters fitting at the same effective undisturbed ground temperature of $T_0 \approx 18.32$°C without heat dissipation to the ambient (i.e., at $\eta = 0$). **Fig. 5** demonstrates the ability of the proposed model to predict the temperature of the heat carrier fluid as function of time.

After ground thermal conductivity, thermal resistance of the borehole is the most important test estimate for the design of a vertical BHE. The borehole resistance values are also estimated from the field data and are plotted versus the time evaluation interval in **Fig. 6**. In fact, Fig. 6 shows that the borehole, filled with thermally enhanced grout, yielded values within the range from 0.151 to 0.185 m°C/W. The estimate of the undisturbed ground temperature (from the three-parameter estimation scheme) varies from 19.4 to 17.9°C for the same time intervals. This range includes the T_0 value used for determination of the model parameter p in **Eq. 13** and **14**. Therefore, the developed method successfully filters out the main part of the cyclic distortions of test estimates caused by the diurnal temperature cycle and smoothens their dependencies on the length of time interval chosen for the assessment.

When neglecting energy losses to the ambient air ($p = 0$), the values of λ calculated from both ILS and FLS models are higher than ones evaluated with the proposed method of suppressing the climatic influence from the TRT data; this is because of the cooling effect. For $\eta \neq 0$ ($p \neq 0$), as well as for $\eta = 0$ ($p = 0$), the comparison between the numerical results of FLS and ILS models applied to the same experimental data shows that, as predicted by Bandos et al. (2009), the effective thermal conductivity value of the ground is overestimated by the ILS model (**Fig. 4**).

5. Conclusions

The ground thermal conductivity has been estimated from the TRT data by modeling a BHE as a finite and infinite line-source of constant heat flow. A method of subtracting the influence of outside perturbations has been developed and applied in the estimation process. The removal of the climatic effect successfully damps the oscillations of the ground conductivity estimates from the test data with increasing length of the time series. Application to the borehole test demonstrates that the atmospheric effect can distort the estimate of ground conductivity by a factor of one-third, while the proposed method estimates ground conductivity to within a 10% interval of the mean value. It has been shown that this proposed method of using the ambient temperature data in the analysis allows suppression of the influence of diurnal atmospheric conditions on the estimates of thermal conductivity and borehole resistance.

Parameter estimation from the test data yields a lower value for ground thermal conductivity when some energy dissipates from the above-ground pipes in the heat injection mode. This holds true for calculations in the framework of of both infinite and finite line-source models.. The results confirm that the finite depth corrections for the mean borehole temperature result in decreasing the ground thermal conductivity estimate from test data and improve accuracy of the evaluation. The proposed method is model-independent and is valid for data analysis with the line-source or cylindrical model for BHE.

Acknowledgments

This paper has been supported by the European Union Commission under projects GROUND-MED FP7-ENERGY-2007-2-TREN-218895, 043340, and Geotrainet - IEE/ 07/581; the Spanish Ministry of Education and Science under projects "Modelado y simulación de sistemas energéticos complejos" (Programa Ramón y Cajal 2005) and ENE2008-00599/CON; by the Government of Valencia under project GV/2008/292; and by PAID-06-09/2734.

References

Austin, W. A., 1998. Development of an In situ System for Measuring Ground Thermal Properties. MS thesis, Oklahoma State University, Stillwater, Oklahoma, 177 pp.

Bandos, T.V., Montero, Á., Fernández, E., Santander, J.L.G., Isidro, J.M., Pérez, J., Fernández de Córdoba, P.J., and Urchueguía, J.F., 2009. Finite line-source model for borehole heat exchangers: Effect of vertical temperature variations. Geothermics 38, 263–270.

Beier, R.A. and Smith, M.D., 2002. Borehole Resistance from Line-Source Model of In situ Tests. American Society of Heating, Refrigerating American Engineers Transactions 108(2), pp. 212–219.

Beier, R.A. and Smith, M.D., 2003. Removing Variable Heat Rate Effects from Borehole Tests. American Society of Heating, Refrigerating American Engineers Transactions 109(2), pp. 463–474.

Beier, R.A., 2008. Equivalent time for interrupted tests on borehole heat exchangers. International Journal of Heating Ventilating, and Airconditioning Research 14, 489–503.

Bose, J. E., Parker, J. D., and McQuiston, F. C., 1985. Design/Data Manual for Closed Loop Ground Coupled Heat Pump Systems. American Society of Heating, Refrigerating, and Air Conditioning Engineers, Atlanta, Georgia, 16 pp.

Carslaw, H. S. and Jaeger, J. C., 1959. Conduction of Heat in Solids. Oxford University Press, New York, NY, 510 pp.

Claesson, J. Eskilson, P., 1988. Conductive heat extraction to a deep borehole, thermal analysis and dimensioning rules. Energy 13, 509– 527.

Eskilson, P., 1987. Thermal Analysis of Heat Extraction Boreholes. PhD dissertation, Department of Mathematical Physics, University of Lund, Lund, Sweden, 264 pp.

Esen, H., and Inalli, M., 2009. In-Situ thermal response test for ground source heat pump system heat exchanger in Elazig, Turkey. Energy and Buildings 41, 395–401.

Florides, G. and, Kalogirou S., 2008. First In-Situ determination of the thermal performance of a U-Pipe borehole heat exchanger in Cyprus. Applied Thermal Engineering 28, 157–163.

Fujii, G., Okubo, H., Nishi, K., Itoi, R., Ohyama, K., and Shibata, K., 2009. An improved thermal response test for U-Tube ground heat exchanger based on optical fiber thermometers. Geothermics 38(4), 399–406.

Gehlin, S. and Hellström, G., 2003. Comparison of Four Models for Thermal Response Test Evaluation. American Society of Heating, Refrigerating American Engineers Transactions 109, pp. 131–142.

Gehlin, S. and Nordell, B., 2003. Determining Undisturbed Ground Temperature for Thermal Response Test. American Society of Heating, Refrigerating American Engineers Transactions 107, pp. 151–156.

Hastie, T., Tibishirani, R., and Friedman, J., 2001. The Elements of Statistical Learning. Springer-Verlag, New York, NY, 536 pp.

Hellström, G., 1991. Thermal Analysis of Duct Storage System. Department of Mathematical Physics, University of Lund, Lund, Sweden, 262 pp.

Ingersoll, L.R., Zohel, O.J., and Ingersoll, A.C., 1954. Heat Conduction with Engineering Geological and Other Applications. University of Wisconsin Press, Madison, Wisconsin, 342 pp.

Javed, S., Fahlén, P., and Claesson, J., 2009. Vertical Ground Heat Exchangers: A Review of Heat Flow Models. In: Proceedings of 11th International Congress on Thermal Energy Storage for Efficiency and Sustainability, Stockholm, Sweden, 8 pp.

Lamarche, L. and Beauchamp, B., 2007. A new contribution to the finite line-source model for geothermal boreholes. Energy and Buildings 39, 188–198.

Lund, J. W., 2000. Ground Source (Geothermal) Heat Pumps. in: Lineau, P. J. (Ed.), Course on Heating with Geothermal Energy: Conventional and New Schemes. World Geothermal Congress Short Courses. Kazuno, Tohuko district, Japan, pp. 1–21.

Marcotte, D. and Pasquier, P., 2008. On the estimation of thermal resistance in borehole thermal conductivity test. Renewable Energy 33, 2407–2415.

Mogensen, P., 1983. Fluid to Duct Wall Heat Transfer in Duct System Heat Storage. In: Proceedings of the International Conference on Surface Heat Storage in Theory and Practice, Stockholm, Sweden, pp. 652–657.

Omer, A.M., 2008. Ground-source heat pump systems and applications. Renewable and Sustainable Energy Reviews 12(2), 344–371.

Philippe, M., Bernier, M., Marchio, D., 2009. Validity ranges of three analytical solutions to heat transfer in the vicinity of single boreholes. Geothermics 38, 407–413.

Reuβ, M., Proell, M., Nordell, J., 2009. IEA ECES-ANNEX 21 THERMAL RESPONSE TEST. In: Proceedings of 11th International Congress on Thermal Energy Storage for Efficiency and Sustainability, Stockholm, Sweden, 8 pp.

Sanner, B., Hellström, G., Spitler, J. Gehlin, S., 2005. Thermal Response Test-Current Status and World-Wide Application. In: Proceedings World Geothermal Congress, Antalya, Turkey, pp. 1436–1445.

Signorelli, S., Bassetti, S., Pahud, D., Kohl, T., 2007. Numerical evaluation of thermal response tests. Geothermics 36, 141–166.

Shonder, J.A., Beck, J.V., 2000. Field Test of a New Method for Determining Soil Formation Thermal Conductivity and Borehole Resistance. American Society of Heating, Refrigerating American Engineers ASHRAE Transactions 106(1), pp. 843–850.

Spitler, J. D., 2000. GLHEPRO: A Design Tool for Commercial Building Ground Loop Heat Exchangers. In: Proceedings of the Fourth International Heat Pumps in Cold Climates Conference, Aylmer, Queb´ec, pp. 1–26.

Urchueguía, J.F., Zacarés, M., Corberán, J.M., Montero, Á, Martos, J., Witte, H., 2008. Comparison between the energy performance of a ground coupled water to water heat pump system and an air to water heat pump system for heating and cooling in typical conditions of the European Mediterranean coast. Energy Conversion and Management 49, pp. 2917–2923.

Witte, H.J.L., van Gelder, G.J., and Spitler, J.D., 2002. In situ measurement of ground thermal conductivity: A Dutch perspective. American Society of Heating, Refrigerating American Engineers ASHRAE Transactions 108, pp. 1–10.

Zeng H., Diao N., Fang Z., 2002. A finite line-source model for boreholes in geothermal heat exchangers. Heat Transfer Asian Research 31, 558–567.

Figure captions

Figure 1. Schematic of field test to measure ground properties.

Figure 2. Daily variations of the air temperature (black line) and the average fluid temperature (gray line) versus the time of the thermal response test at constant heat injection rate.

Figure 3. Time variation of the measured total heat rate, Q_t (gray line) and variable heat rate, q_zH, transferred to ground (black line). Q_{air} calculated with the fitting parameter η= 0.006 corresponding to 5.5% heat losses (p = 0.055) to ambient air (dashed black line).

Figure 4. Comparison between dependence of thermal conductivity on the time interval length from the ILS (gray line) and FLS (black line) models for the same test data. Estimates of thermal conductivity are from the ILS and FLS models when the end of the evaluation interval is fixed while its starting point increases: (i) without outside heat losses to the ambient air (p = 0, η = 0) and (ii) with 5.5% heat losses (p = 0.055, η = 0.006) to the ambient air.

Figure 5. Measured (gray line) and calculated mean fluid temperature versus the natural log of time (hrs) from two FLS models with (solid black line) and without (p = 0, dashed black line) external heat dissipation for the converged test parameters values.

Figure 6. Comparison between dependence of borehole thermal resistance on the time interval length from the ILS (black line) and FLS (gray line) models for the same test data assuming 5.5% heat losses (p = 0.055, η = 0.006) to the ambient. Estimates of BHE thermal resistance are from the ILS and FLS models when the end of the evaluation interval is fixed while its starting point increases

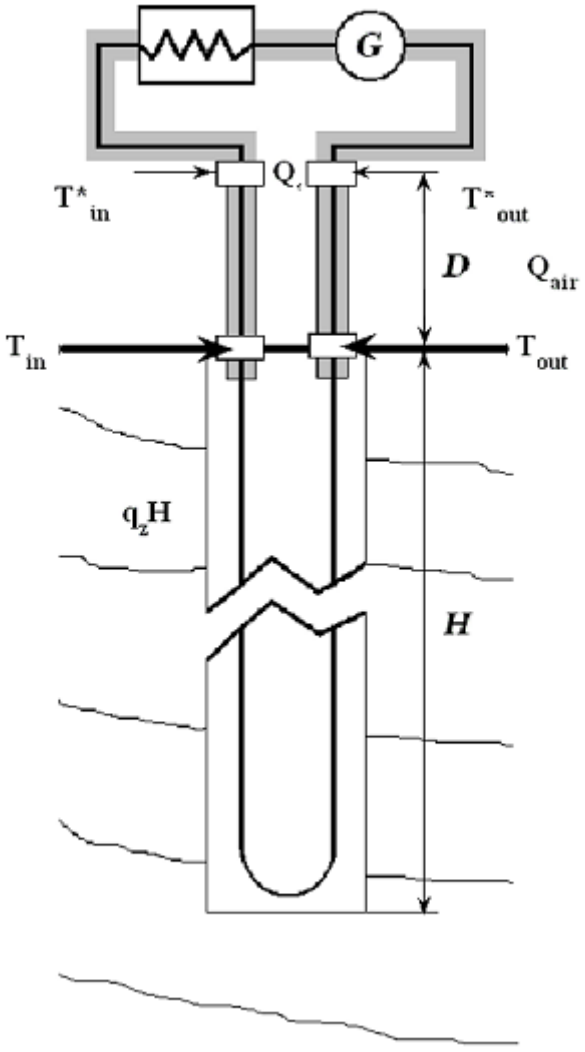

FIGURE 1

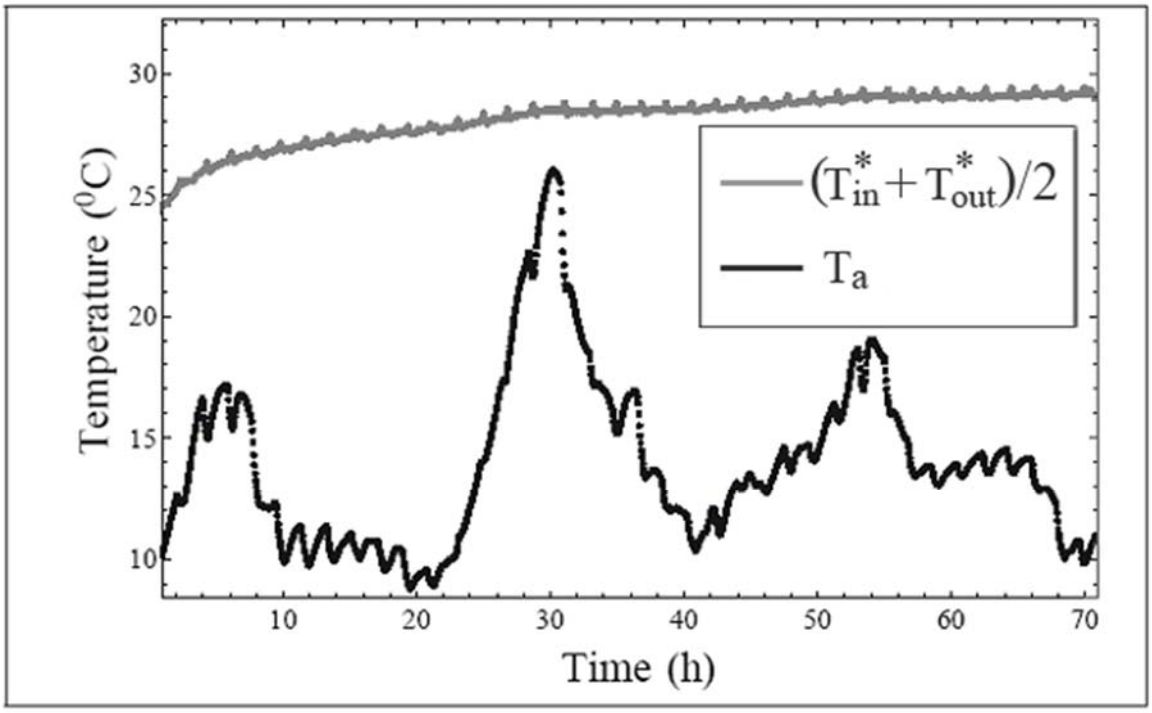
Temperature (^{0}C)
Time (h)
$(T^*_{in}+T^*_{out})/2$
T_a
30
25
20
15
10
10
20
30
40
50
60
70

FIGURE 2

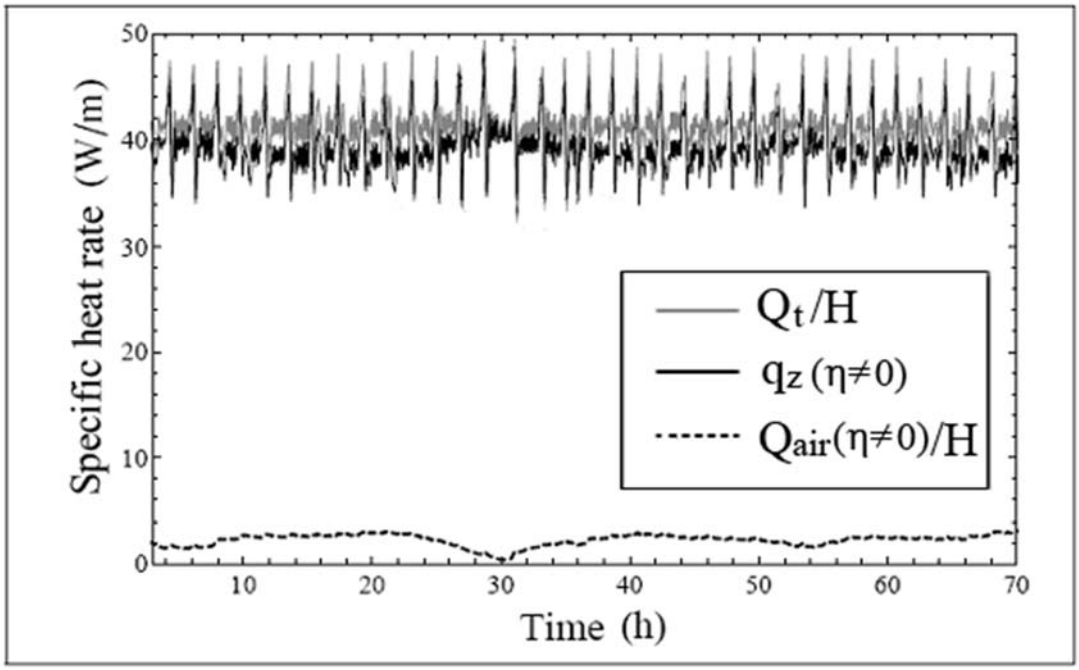
Specific heat rate (W/m)
Time (h)
Qt/H
qz (η≠0)
Qair(η≠0)/H
0
10
20
30
40
50
60
70

FIGURE 3

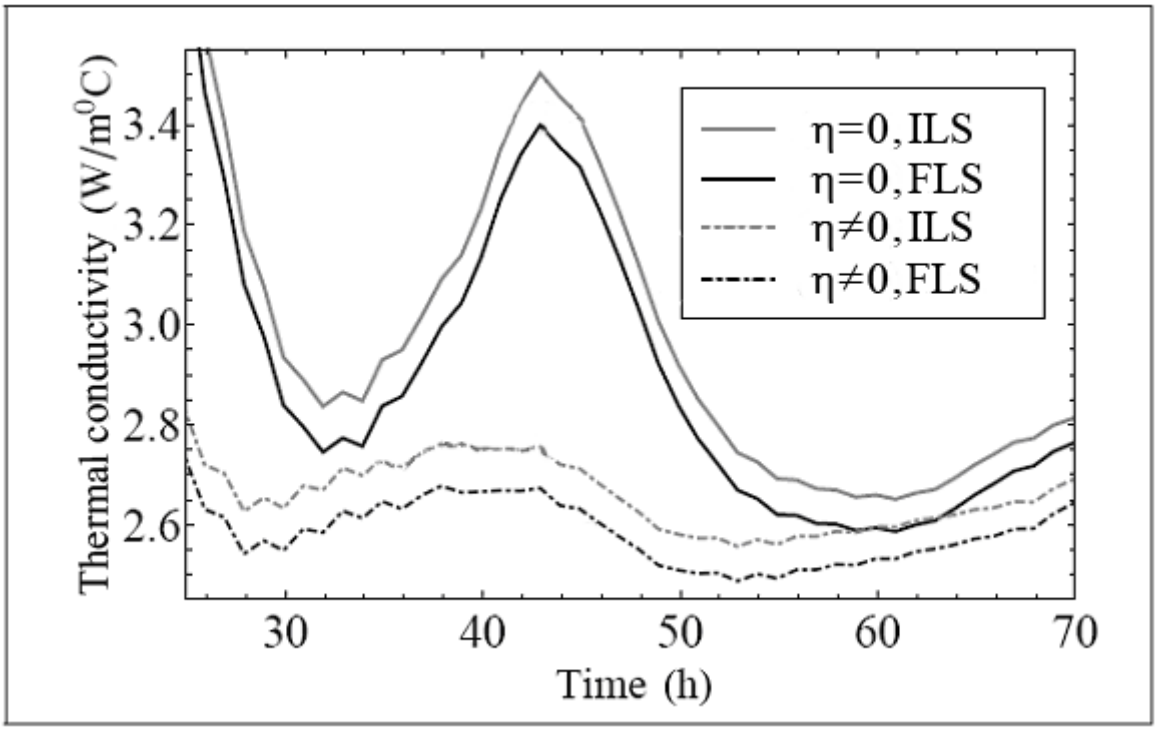
Thermal conductivity (W/m^{0}C)
3.4
3.2
3.0
2.8
2.6
30
40
50
60
70
Time (h)
η=0,ILS
η=0,FLS
η≠0,ILS
η≠0,FLS

FIGURE 4

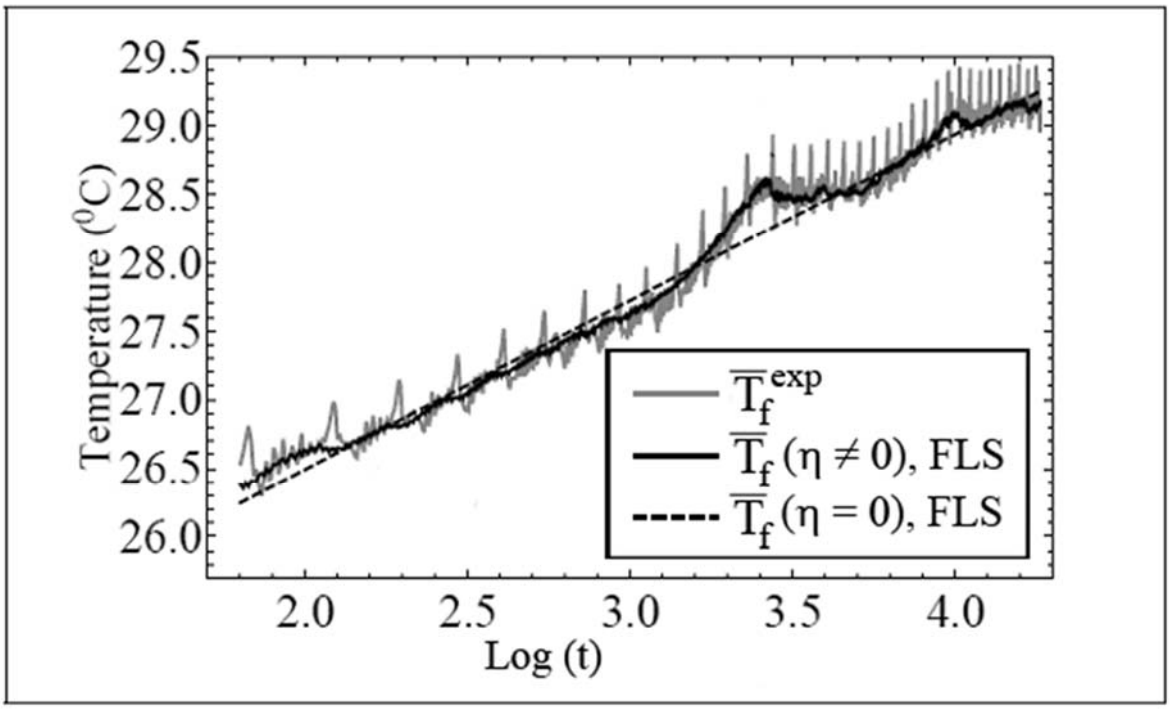
29.5
29.0
28.5
28.0
27.5
27.0
26.5
26.0
Temperature (°C)
2.0
2.5
3.0
3.5
4.0
Log (t)
$\overline{T}_f^{exp}$
$\overline{T}_f(\eta \neq 0)$, FLS
$\overline{T}_f(\eta = 0)$, FLS

FIGURE 5

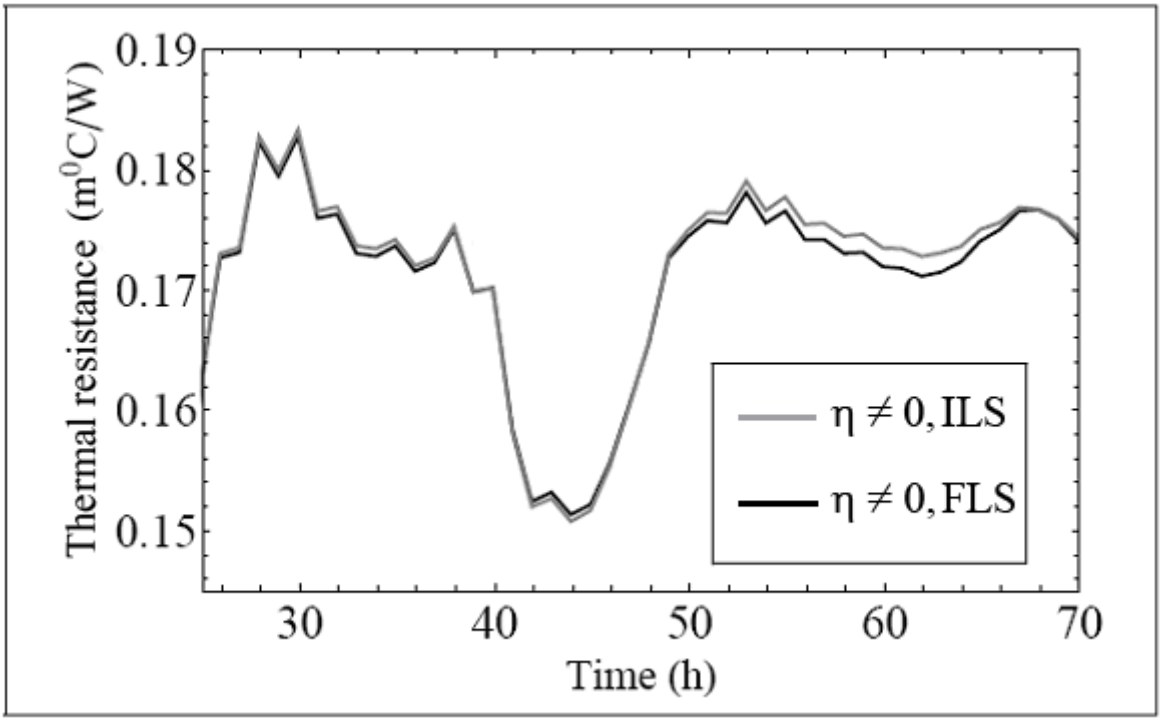
Thermal resistance (m^0C/W)
0.19
0.18
0.17
0.16
0.15
30
40
50
60
70
Time (h)
$\eta \neq 0$, ILS
$\eta \neq 0$, FLS

FIGURE 6